On stabilized finite element methods based on the Scott–Zhang projector. Circumventing the inf–sup condition for the Stokes problem

Santiago Badia *

Centre Internacional de Mètodes Numèrics en Enginyeria (CIMNE), Parc Mediterrani de la Tecnologia, Esteve Terrades 5, 08860 Castelldefels, Spain
Universitat Politecnica de Catalunya, Jordi Girona 1-3, Edifici C1, 08034 Barcelona, Spain

ARTICLE INFO

ABSTRACT

In this work we propose a stabilized finite element method that permits us to circumvent discrete inf–sup conditions, e.g. allowing equal order interpolation. The type of method we propose belongs to the family of symmetric stabilization techniques, which are based on the introduction of additional terms that penalize the difference between some quantities, i.e. the pressure gradient in the Stokes problem, and their finite element projections. The key feature of the formulation we propose is the definition of the projection to be used, a non-standard Scott–Zhang projector that is well-defined for $L^1(\Omega)$ functions. The resulting method has some appealing features: the projector is local and nested meshes or enriched spaces are not required.

1. Introduction

Many physical problems in science and engineering are modeled with partial differential equations without a coercivity property, e.g. the (Navier–)Stokes equations for incompressible flows, Darcy's problem for flux in porous media, and some versions of the Maxwell equations. At the continuous level, these saddle-point problems are well posed by virtue of some inf–sup condition. As model problem, let us consider Stokes' system on a bounded open domain Ω with homogeneous boundary conditions:

$$-v\Delta u + \nabla p = f, \quad \nabla \cdot u = 0, \quad u|_{\partial\Omega} = 0, \tag{1}$$

where u is the velocity, p the pressure, v the fluid viscosity and f the body force. Using standard notation, we can state the problem in weak form: find $(u, p) \in H_0^1(\Omega) \times L_0^2(\Omega)$ such that

$$c(u, p, v, q) := v(\nabla u, \nabla v) - (p, \nabla \cdot v) + (q, \nabla \cdot u) = \langle f, v \rangle =: \ell(v) \tag{2}$$

for any $(v, q) \in H_0^1(\Omega) \times L_0^2(\Omega)$. For the Stokes problem, pressure stability relies on the following inf–sup condition: for any $p \in L_0^2(\Omega)$, there exists a $v_p \in H_0^1(\Omega)$ with unit norm such that $\beta\|p\| \geqslant (p, \nabla \cdot v_p)$, for some $\beta > 0$. Unlike coercivity, inf–sup conditions are not inherited by sub-spaces of functions, complicating Galerkin approximations. We have to explicitly build finite element (FE) spaces that satisfy discrete versions of the inf–sup conditions, and appealing choices such as equal-order interpolation for all the

unknowns cannot be used [8]. The situation is slightly more involved in general, since the well-posedness of saddle-point problems only requires coercivity on the kernel of the constraint operator, e.g. the Maxwell and Darcy problems [14].

The use of inf–sup stable formulations can be particularly impractical in multi-physics simulations of saddle-point systems, i.e. inductionless magnetohydrodynamics (MHD) (coupling Stokes and Darcy-type problems, see [21]) or incompressible visco-resistive MHD (coupling Stokes and Maxwell-type problems, see [3]). This approach requires different FE spaces for the different unknowns [22], complicating the integration subroutines and the matrix graph (a different graph for every block of the full matrix is needed). In other situations, in which different asymptotic limits of the problem (in terms of the physical parameters) lead to different saddle-point systems, e.g. the Brinkman model for creeping flow in porous media, the inf–sup stable approximation cannot lead in general to unconditional stability, since different limits require different FE spaces (see [1]).

Alternatively, we can consider stabilized FE techniques, which consist in the introduction of additional (stabilization) terms that provide the numerical method with the proper stability without the need to satisfy discrete inf–sup conditions. Initially, the stabilization terms were based on the residual at FE interiors, as in the popular Galerkin/least-squares (GLS) method [16] and the improved Variational Multiscale (VMS) method [17] proposed by Hughes and co-workers. Let us consider a partition $\mathcal{T}_h$ of Ω into tetrahedra/hexahedra, denoted by K, and conforming FE spaces $V_h \times Q_h \subset H_0^1(\Omega) \times L_0^2(\Omega)$. The stabilized methods GLS ($\theta = -1$) and VMS ($\theta = 1$) read as:

* Address: Universitat Politecnica de Catalunya, Jordi Girona 1-3, Edifici C1, 08034 Barcelona, Spain.
E-mail address: sbadia@cimne.upc.edu

$$c(u_h, v_h, p_h, q_h) + \sum_{K \in \mathcal{T}_h} \delta_K(-\Delta u_h + \nabla p_h, \theta \Delta v_h + \nabla q_h)_K$$

$$= \ell(v_h) + \sum_{K \in \mathcal{T}_h} \delta_K \langle f, \theta \Delta v_h + \nabla q_h \rangle_K, \tag{3}$$

where δ_K is a numerical parameter to be defined later. These methods allow equal-order interpolation, are consistent and exhibit optimal convergence rates. On the other side, they are usually criticized for giving unphysical pressure boundary layers [5], for the additional cost involved in the evaluation of higher order derivatives and the weak inconsistency for first order approximations [18], the fact that the forcing term is also affected by the stabilization and the hard extension to transient problems [13], usually carried out via expensive space–time FEs (see e.g. [24]). Probably, the main shortcoming of GLS, VMS and related residual-based formulations is manifested when dealing with multi-physics applications. These stabilized FE formulations include a large number of additional coupling terms, which fill blocks that are zero for the Galerkin method; see [21,3] for MHD applications. Another important problem related to these methods is the fact that they destroy the skew-symmetric form of the off-diagonal blocks (stabilized gradient and divergence matrix) in the Navier–Stokes and MHD systems, making pressure-segregation (fractional step) methods to lose their unconditional stability (see [4]).

The introduction of symmetric stabilization techniques represented one step further in the improvement of FE stabilization techniques, since they solve all the problems commented above. Instead of considering residual-based terms, these methods introduce penalty terms over the difference between some quantities, i.e. the pressure gradient for the Stokes problem, and their projections. This family of methods does not perturb the right-hand side of the problem, and stabilizes the bilinear form as follows:

$$c(u_h, v_h, p_h, q_h) + \sum_{K \in \mathcal{T}_h} \delta_K(\nabla p_h - \pi_h(\nabla p_h), \nabla q_h - \pi_h(\nabla q_h))_K = \ell(v_h),$$

where $\pi_h(\cdot)$ is a FE projector; different definitions for $\pi_h(\cdot)$ lead to different techniques. The resulting method is only weakly consistent, i.e. the stabilization term does not cancel for the exact solution but vanishes as the mesh size $h \searrow 0$ in such a way that optimal convergence is kept. Motivated by the inherited stability of fractional step methods, Codina and Blasco provided in their pioneering work [12] the first algorithm of this kind, based on the $L^2(\Omega)$-orthogonal projector, coined orthogonal subscales (OSS). Unfortunately, this projector is global, i.e. the stabilization term leads to a dense matrix. Certainly, the method is never computed this way, and the projection is usually sent to the right-hand side of the linear system. In case of solving transient problems, it can simply be treated explicitly. In those situations, for reasonably small time step sizes, the OSS method has perfect sense and it is an effective and simple algorithm, since the CPU cost per time step used for the computation of the global projections in negligible. On the contrary, to send the projection term to the right-hand side, and make it implicit via Richardson iterations (usually merged with nonlinear iterations [11]) is not advisable unless a very small time-step size is used, since it can drastically increase the number of nonlinear iterations or simply diverge; this approach is even harder to justify for linear problems as the Stokes system. An alternative consists in dealing with the exact matrix, explicitly solving the mass matrix systems for the projection evaluations at every iteration of an external Krylov solver. This approach is hard to implement and prevent us to use direct solvers, and by extension substructuring domain decomposition techniques with exact local solvers [25].

Becker and Braack envisaged in [5] an original way to avoid the global projections in [12]. Their method was later called local projection stabilization (LPS). The price to pay is a tighten requirement over the mesh partitions: specific hierarchical meshes were

needed, since the method is based on the definition of fine and coarse FE spaces. On the other hand, the projection is not over the original FE space, as in [12], but on a discontinuous space of functions. The original LPS formulation has been lately denoted as two-level LPS, due to the requirement of two nested meshes for the definition of the stabilization terms. A one-level LPS formulation has also been designed [19], in which the fine space is attained with an enrichment of the coarse one via additional functions of bubble type. This way, we can eliminate the stringent mesh requirement but now a particular type of enriched FE spaces must be used.

The development of stabilized FE methods that allows one to circumvent inf–sup conditions has been almost entirely developed for the Stokes problem and the nonlinear Navier–Stokes equations. The extension to problems that only present coercivity in the kernel of the constraint operator is more recent. We refer to [2] for a detailed exposition of VMS and symmetric projection stabilization schemes for Darcy's and Maxwell's problems.

The purpose of this work is to present a new method, based on a particular $L^1(\Omega)$ Scott–Zhang projector that shares all the aforementioned benefits of symmetric stabilization techniques as well as: *only local projections* are required, *no assumption over the mesh partition* (e.g. nested meshes) is needed and *no assumption over the FE spaces* (e.g. equal-order Lagrangian FEs can be used without additional enrichment) is needed.

In Section 2, we introduce some notation, as well as the definition of the method and implementation aspects. Section 3 is devoted to the numerical analysis of the algorithm, both stability and *a priori* error estimates. Some numerical tests are presented in Section 4. Finally, we draw some conclusions in Section 5.

2. Definition of the method

Let us consider the Stokes problem (2) for an open, bounded polyhedral domain Ω in $\mathbb{R}^d$, where $d = 2, 3$ is the space dimension. We will use standard notation for Sobolev spaces (see [7]). In particular, the $L^2(\omega)$ scalar product will be denoted by $(\cdot, \cdot)_\omega$ for some $\omega \subset \Omega$, but the domain subscript is omitted for $\omega \equiv \Omega$ (analogously for the duality pairing $\langle \cdot, \cdot \rangle$). The $L^2(\Omega)$ norm is denoted as $\| \cdot \|$. We will define the velocity and pressure spaces as $V_0 \equiv H_0^1(\Omega)$ and $Q \equiv L_0^2(\Omega)$, endowed with the norms $\|v\|_V := v^{\frac{1}{2}}\|\nabla v\|$ and $\|q\|_Q := v^{-\frac{1}{2}}\|q\|$, properly scaled with the fluid viscosity v. $C^0(\bar{\Omega})$ denotes the space of continuous functions. We will omit the d superscript in vector-valued functional spaces.

Let us consider now a partition $\mathcal{T}_h$ of Ω into d-simplices, quadrilaterals ($d = 2$) or hexahedra ($d = 3$) where every $K \in \mathcal{T}_h$ is the image of a reference element $\widehat{K}$ through an affine mapping $F_K : \widehat{K} \to K$ (see [9, Chp. 2]); we can assume that every edge of $\widehat{K}$ has length one. $P_r(\widehat{K})$ is the space of complete polynomials of degree r on $\widehat{K}$. For d-simplicial FE partitions, we define the space of element-wise discontinuous functions

$$D_h := \{v_h : v_h|_K \circ F_K \in P_r(\widehat{K}), \ K \in \mathcal{T}_h\}.$$

The continuous FE spaces are obtained by enforcing continuity, namely $V_h := D_h \cap C^0(\bar{\Omega})$ and $Q_h := D_h \cap C^0(\bar{\Omega}) \cap L_0^2(\Omega)$ for the velocity and pressure respectively. We will also make use of the FE space with null trace $V_{h,0} := V_h \cap H_0^1(\Omega)$. The order of approximation r to be used for velocity and pressure approximations can be different. For quadrilaterals and hexahedra, the spaces are obtained by replacing $P_r(\widehat{K})$ by $Q_r(\widehat{K})$, the space of polynomials with maximum degree r in each reference space coordinate on $\widehat{K}$.

For the FE space V_h we denote by $\mathcal{N}_h$ the set of all interpolation nodes related to $\mathcal{T}_h$ and by $\{\phi^a\}_{a \in \mathcal{N}_h}$ the corresponding nodal basis of V_h. We also denote by $\mathcal{N}_h(K)$ the set of all nodes that belong to a FE K. Continuous FE functions can be written as $v_h = \sum_{a \in \mathcal{N}_h} v_h^a \phi^a(\mathbf{x})$, where v_h^a denotes the nodal value of v_h corresponding to a. Analo-

gously, $\{\phi^a(\mathbf{x})|_K\}_{K \in \mathcal{T}_h, a \in \mathcal{N}_h(K)}$ is the basis for D_h and discontinuous FE functions are written as $v_h = \sum_{K \in \mathcal{T}_h} \sum_{a \in \mathcal{N}_h(K)} v_h|_K^a \phi^a(\mathbf{x})|_K$, where $v_h|_K^a$ is the value of v_h in the node a at element K. Further, we denote the adjacency list $\mathcal{A}_h^{\mathrm{nd}}(a)$ of a node $a \in \mathcal{N}_h$ as the set of nodes $c \in \mathcal{N}_h$ such that $a, c \in \mathcal{N}_h(K)$ for some $K \in \mathcal{T}_h$, i.e. the set of neighbor nodes. On the other hand, $\mathcal{A}_h^{\mathrm{el}}(a)$ is the set of elements $K \in \mathcal{T}_h$ such that $a \in \mathcal{N}_h(K)$, i.e. the set of neighbor elements.

2.1. Nodal projection stabilization

At this point, let us introduce a variant of the Scott–Zhang projector [23] which is well-defined for $L^1(\Omega)$ functions. The analysis in [23] does apply for this projector even though it is not the standard version, because it does not keep homogeneous boundary conditions (see Remark 1). We can build a node-to-element map $\kappa : \mathcal{N}_h \to \mathcal{T}_h$; for interior nodes there is only one choice, two choices for nodes on faces and possibly more for nodes on edges or vertices. Following [23], for any $a \in \mathcal{N}_h$ there is only one dual function $\psi^a \in P_r(K)$ (analogously for $Q_r(K)$) such that

$$\int_{\kappa(a)} \psi^a(\mathbf{x})\phi^b(\mathbf{x}) d\mathbf{x} = \delta_{ab}, \quad \text{for any } b \in \mathcal{N}_h(\kappa(a)). \tag{4}$$

Now, we construct the projector $i_h : L^1(\Omega) \to V_h$ as follows:

$$i_h(v) := \sum_{a \in \mathcal{N}_h} \phi^a(\mathbf{x}) \int_{\kappa(a)} \psi^a(\mathbf{x}) v(\mathbf{x}) d\mathbf{x}. \tag{5}$$

Let us also define $i_h^\perp(v) := v - i_h(v)$. With this notation, we are in position to state the proposed algorithm: find $(u_h, p_h) \in V_{h,0} \times Q_h$ such that:

$$c_h(u_h, v_h, p_h, q_h) := c(u_h, v_h, p_h, q_h) + (i_h^\perp(\nabla p_h), i_h^\perp(\nabla q_h))_\delta$$
$$= \ell(v_h) \quad \text{for any } (v_h, q_h) \in V_{h,0} \times Q_h, \tag{6}$$

$$\text{with} \quad (\cdot, \cdot)_\delta := \sum_{K \in \mathcal{T}_h} \delta_K (\cdot, \cdot)_K, \quad \delta_K := \frac{c_\delta h_K^2}{\nu}. \tag{7}$$

$\delta_K : \mathcal{T}_h \to \mathbb{R}$ is the so-called stabilization parameter, c_δ being an algorithmic constant independent of h. A variable viscosity can easily be handled, e.g. by taking $\nu_K = \int_K \nu(\mathbf{x}) d\mathbf{x}$, but a constant viscosity is assumed for the sake of clarity. We will refer to this method as nodal projection stabilization (NPS), since $i_h(\cdot)$ is a local projection defined node-wise. The method clearly belongs to the family of symmetric stabilization techniques.

Motivated by the stability analysis in the next section, we consider an alternative NPS scheme (6) by introducing a nodal definition of the stabilization parameter, denoted by δ_a. Given a (generally discontinuous) FE element function $v_h \in D_h$, we define $\delta(v_h)(\mathbf{x}) := \sum_{K \in \mathcal{T}_h} \sum_{a \in \mathcal{N}_h} \delta_a v_h|_K^a \phi|_K^a(\mathbf{x}) \in D_h$. We define $\delta^{\frac{1}{2}}(\cdot)$ analogously, by replacing δ_a with $\delta_a^{\frac{1}{2}}$. Let us remark that $\delta(\cdot)$ keeps continuity and homogeneous boundary conditions, i.e. given $v_h \in V_h$, $\delta(v_h) \in V_h$ (idem for $V_{h,0}$). The method consists in (6) with a different definition of the δ-product:

$$(\cdot, \cdot)_\delta := (\delta^{\frac{1}{2}}(\cdot), \delta^{\frac{1}{2}}(\cdot)), \quad \delta_a := \frac{c_\delta h_a^2}{\nu}, \quad \text{with } h_a := h_{\kappa(a)}. \tag{8}$$

Alternative definitions of h_a are possible (see Lemma 4). In this case, the stability analysis in Theorem 6 becomes slightly simpler.

This method is strongly related to the OSS formulation proposed by Codina and Blasco in [12], which uses instead the $L^2(\Omega)$ projector $\pi_h(v) \in V_h$, defined as the solution of

$$(\pi_h(v), w_h) = (v, w_h), \quad \text{for any } w_h \in V_h. \tag{9}$$

However, this projector is not local, since it involves the solution of a global linear system with a Gramm matrix. On the other hand, LPS techniques share with NPS the fact that the projections are local, but the projectors are not defined over V_h and they require additional assumptions over the mesh or FE spaces to be used. We refer to [5,19] for a detailed definition of LPS techniques.

Remark 1. For the OSS formulation, it has been proposed to use the $L^2(\Omega)$ projector $\pi_{h,0}$ onto $V_{h,0}$ instead, i.e. the solution $\pi_{h,0}(v) \in V_{h,0}$ of

$$(\pi_{h,0}(v), w_h) = (v, w_h), \quad \text{for any } w_h \in V_{h,0}. \tag{10}$$

It does not require Assumption 5 below to hold but can exhibits pressure boundary layers. Analogously for NPS, we can consider a projector $i_{h,0}$ onto $V_{h,0}$. It can be accomplished by modifying the projector (5) at nodes $a \in \partial\Omega$ only. For these boundary nodes, we can use the technique in [23], based on edge integrals, since $i_{h,0}$ is only applied over ∇Q_h functions, which have well-defined traces on $\partial\Omega$. Alternatively, we can use the modification proposed by Girault and Lions [15], which simply consists in taking $i_h(\nabla q_h)^a$ equal to zero for boundary nodes. In fact, for the FE functions to be projected in method (6) these two techniques are equivalent.

2.2. Implementation aspects

In this section we will assume the equal-order interpolation case for the sake of clarity. Let us discuss how to implement the stabilization term in (6). The key ingredient is the computation of $i_h(\nabla p_h)$. By linearity we only need to consider the projection of the basis $\{\nabla \phi^a\}_{a \in \mathcal{N}_h}$ of the discontinuous FE space ∇Q_h. We have the following result.

Lemma 2. Let us assume that $r_p \leqslant r_u + 1$, where r_u and r_p are the order of approximation for the velocity and pressure respectively. Then, the matrix associated to the term $(i_h(\nabla \cdot), i_h(\nabla \cdot)) : Q_h \to Q_h'$, can be built as follows: for any $a, b \in \mathcal{N}_h$

$$(i_h(\nabla \phi^a), i_h(\nabla \phi^b)) = \sum_{c \in \mathcal{A}_h^{\mathrm{nd}}(a)} \sum_{d \in \mathcal{A}_h^{\mathrm{nd}}(b)} \nabla \phi^a|_{\kappa(c)}^c \cdot \nabla \phi^b|_{\kappa(d)}^d (\phi^c, \phi^d).$$

Proof. By the definition of the projector (5), we have: for any $a \in \mathcal{N}_h$

$$i_h(\nabla \phi^a) = \sum_{c \in \mathcal{A}_h^{\mathrm{nd}}(a)} i_h(\nabla \phi^a)^c \phi^c, \quad \text{where} \quad i_h(\nabla \phi^a)^c$$
$$= \int_{\kappa(c)} \nabla \phi^a(\mathbf{x})\psi^c(\mathbf{x}) d\mathbf{x}. \tag{11}$$

We have used the simple fact that $\nabla \phi^a|_{\kappa(c)} = 0$ if $c \notin \mathcal{A}_h^{\mathrm{nd}}(a)$, since $a \notin \kappa(c)$ and so $\nabla \phi^a|_{\kappa(c)} = 0$. Now, let us use the fact that, given a FE K, for any $q_h \in Q_h$ there exists a $v_h \in V_h$ such that $\nabla q_h|_K = v_h|_K$. This is true since $r_p \leqslant r_u + 1$. Then, we can write $\nabla \phi^a|_K = \sum_{b \in \mathcal{N}_h(K)} \nabla \phi^a|_K^b \phi^b|_K$. Using this result in (11) and the definition of the dual functions in (4) we readily get:

$$i_h(\nabla \phi^a)^c = \sum_{b \in \mathcal{N}_h(\kappa(c))} \int_{\kappa(c)} \nabla \phi^a|_{\kappa(c)}^b \phi^b(\mathbf{x}) \psi^c(\mathbf{x}) d\mathbf{x}$$
$$= \nabla \phi^a|_{\kappa(c)}^c, \quad \text{for } c \in \mathcal{A}_h^{\mathrm{nd}}(a)$$

and $i_h(\nabla \phi^a)^c = 0$ otherwise. It proves the theorem. $\square$

The inequality $r_p \leqslant r_u + 1$ will naturally be satisfied. The cases of interest are $r_u = r_p$ (for implementation simplicity) or $r_u = r_p + 1$ (from a priori estimates, see Corollary 9). Otherwise, we should simply use formula (5).

In terms of implementation, it is better to build the stabilization terms as indicated in Algorithm 1 (for the most usual element-based integration/assembly); the equivalence is easily checked. Algorithm 1 implements the stabilization matrix for method (6). We can still implement this algorithm in different ways, depending on the treatment of $\nabla \phi^a|_{\kappa(c)}^c$. We can consider to store this array, which has the size of the velocity unknowns array times the number of nodes per element, i.e. for linear simplicial FEs this factor is

$d + 1$. This memory usage is acceptable in an implicit FE code compared to preconditioned solver requirements and it is well-suited for parallelization. Otherwise, it can be computed every time is used, with a slight growth of the operation counter. Finally let us note that we are not required to store it for interior nodes, and that vertex-based and edge-based integration algorithms could be considered instead.

Algorithm 1: Assembly of the pressure stabilization matrix S in scheme (6) (equal-interpolation case)

For every $K \in \mathcal{T}_h$:
    Compute δ_K
    For every c, $d \in \mathcal{N}_h(K)$:
        Compute
    $\int_K \phi^c(\mathbf{x})\phi^d(\mathbf{x})d\mathbf{x}$, $\int_K \nabla\phi^c(\mathbf{x}) \cdot \nabla\phi^d(\mathbf{x})d\mathbf{x}$, $\int_K \phi^c(\mathbf{x})\nabla\phi^d(\mathbf{x})d\mathbf{x}$
        Assemble $S_{cd} \leftarrow S_{cd} + \delta_K \int_K \nabla\phi^c(\mathbf{x}) \cdot \nabla\phi^d(\mathbf{x})d\mathbf{x}$
        For every $a \in \mathcal{N}_h(\kappa(c))$:
            $S_{ad} \leftarrow S_{ad} - \delta_K \nabla\phi^a|_{\kappa(c)}^c \cdot \int_K \phi^c(\mathbf{x})\nabla\phi^d(\mathbf{x})d\mathbf{x}$,
            $S_{da} \leftarrow S_{da} - \delta_K \nabla\phi^a|_{\kappa(c)}^c \cdot \int_K \phi^c(\mathbf{x})\nabla\phi^d(\mathbf{x})d\mathbf{x}$
        For every $a \in \mathcal{N}_h(\kappa(c))$ and $b \in \mathcal{N}_h(\kappa(d))$:
            $S_{ab} \leftarrow S_{ab} + \delta_K \nabla\phi^a|_{\kappa(c)}^c \cdot \nabla\phi^b|_{\kappa(d)}^d \int_K \phi^c(\mathbf{x})\phi^d(\mathbf{x})d\mathbf{x}$

Remark 3. In principle, we could consider the Clément interpolant [10] as an alternative to the Scott–Zhang projector (5), since this interpolation is still local. However, the Clément interpolant is not a projection and does not satisfy homogeneous boundary conditions, in case it is required. The fact that it is not a projector has some undesired effects, e.g. the resulting method does not pass a patch test. That is to say, for an exact solution $u \in V_h$, the FE solution u_h differs from u in general. Further, let us show in Fig. 1 the stencil for a FE, in the worst-case and best-case scenario, as well as the stencil for Clément's interpolant. It can be observed in Fig. 1 that Clément's interpolant leads to a wider stencil of the resulting matrix (a node is coupled to its neighbors' neighbors). These facts motivated the introduction of the Scott–Zhang-type projector (5).

3. Numerical analysis

In this section, we analyze the stability and accuracy of the numerical method (6) for both (7) and (8) versions of the

stabilization term. Let h_K denote the diameter of $K \in \mathcal{T}_h$ and $h := \max_{K \in \mathcal{T}_h} h_K$. We assume a non-degenerate partition: there exists a constant $\sigma \in (1, \infty)$ independent of h such that $\max_{K \in \mathcal{T}_h} \frac{h_K}{\rho_K} \leqslant \sigma$, where ρ_K denotes the radius of the largest closed ball contained in $\overline{K}$. The analysis is simpler for regular partitions, i.e. $\min_{K \in \mathcal{T}_h} \rho_K \geqslant \sigma h$. We will make use of the local inverse estimate

$$\|\nabla v_h\|_K \leqslant c_i h_K^{-1} \|v_h\|_K, \quad \text{for any } K \in \mathcal{T}_h, \tag{12}$$

where $c_i > 0$ can depend on σ (as other constants defined below) but not on h. Further, we use the general approximation theory of the Scott–Zhang projector. Let $v \in W_p^k(\Omega)$ and $0 \leqslant s \leqslant k \leqslant r + 1$: there exists $c_e > 0$ independent of h such that

$$\|v - i_h(v)\|_{W_p^s(K)} \leqslant c_e h_K^{k-s} \|v\|_{W_p^k(S_K)}, \quad \left(\sum_{K \in \mathcal{T}_h} \|v - i_h(v)\|_{W_p^s(K)}^p \right)^{\frac{1}{p}}$$
$$\leqslant c_e h^{k-s} \|v\|_{W_p^k(\Omega)}, \tag{13}$$

where S_K is a domain made of the elements neighboring K (see [6]) and r denotes the order of approximation of the corresponding FE space. The global estimate holds for non-degenerate partitions only. The same estimates hold for $i_{h,0}$ (the interpolant that keeps null traces) as soon as $v \in H_0^1(\Omega)$.

Finally, the symbol $\lesssim$ is used to denote $<$ up to a positive constant independent of h (idem for $\gtrsim$ and $\approx$).

3.1. Stability results

First, we consider some technical results that will allow us to accommodate the analysis for non-degenerate partitions. We can easily check that $n_\sigma^a := \text{card}(\mathcal{A}_h^{el}(a))$ (the maximum number of elements around a) is bounded, depends on σ and a but is independent of h. In fact, we can also find a global integer $n_\sigma := \max_{a \in \mathcal{N}_h} n_\sigma^a$ independent of h.

Given two elements K_1, $K_2 \in \mathcal{A}_h^{el}(a)$, we can always find a sequence of elements

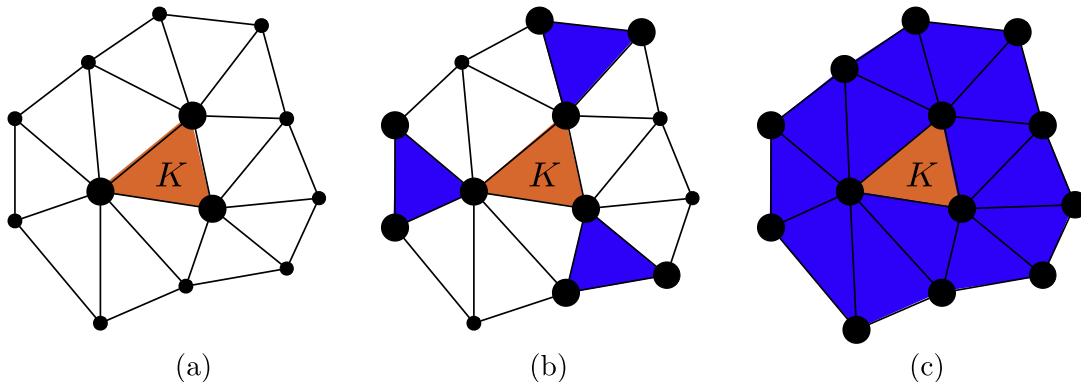$$\mathcal{P}_h(a, K_1, K_2) = \{K_1 \equiv K_{12}^1, K_{12}^2, \dots, K_{12}^m \equiv K_2\} \subset \mathcal{A}_h^{el}(a)$$
$$\text{where } m \leqslant n_\sigma^a,$$

such that K_{12}^i and K_{12}^{i+1} ($i = 1, \dots, m-1$) share an edge (for $d = 2, 3$). We have the following lemma.

Lemma 4. Given a non-degenerate partition $\mathcal{T}_h$, for every node $a \in \mathcal{N}_h$, there exists $h_a > 0$ such that:

$$\sigma^{-\bar{n}_\sigma^a + 1} h_K \leqslant h_a \leqslant \sigma^{\bar{n}_\sigma^a - 1} h_K, \quad \text{for any } K \in \mathcal{A}_h^{el}(a),$$

Fig. 1. Stencil related to the stabilization term $\sum_{a,b \in \mathcal{N}_h(K)} \int_K i_h^\perp(\nabla\phi^a) i_h^\perp(\nabla\phi^b)d\mathbf{x}$ for a given FE element K (in red). The big nodes are those coupled due to this term, and the blue elements are those needed to compute it. We consider three situations: (a) the Scott–Zhang projector (5) in the best case scenario ($K \equiv \kappa(n_1) \equiv \kappa(n_2) \equiv \kappa(n_3)$, where $\{n_i\}_{i=1,2,3}$ is the set of nodes on element K), (b) the same projector in the worst case scenario (where all these FEs are different) and (c) the Clément interpolant. (For interpretation of the references to colour in this figure legend, the reader is referred to the web version of this article.)

where

$$\tilde{n}_\sigma^a(K_i) := \max_{K_j \in \mathcal{A}_h^{el}(a)} \operatorname{card}(\mathcal{P}_h(a, K_i, K_j)), \quad \tilde{n}_\sigma^a := \min_{K_i \in \mathcal{A}_h^{el}(a)} \tilde{n}_\sigma^a(K_i) \leqslant n_\sigma^a.$$

Proof. Suppose the affine mapping $F_K(\tilde{\mathbf{x}}) = B\tilde{\mathbf{x}} + \mathbf{x}_0$. Given two elements K_1, K_2 sharing an edge, denoted by E, we can easily prove (see [9, Th. 3.1.3]):

$$|B_{K_i}^{-1}|^{-1} \leqslant \operatorname{meas}(E) \leqslant |B_{K_i}|, \quad |B_{K_i}| \leqslant h_{K_i}, \quad |B_{K_i}^{-1}| \leqslant \rho_{K_i}^{-1}, \quad \text{for } i = 1, 2.$$

Therefore, we get $\sigma^{-1}h_{K_1} \leqslant h_{K_2} \leqslant \sigma h_{K_1}$. Now, let us take $K_1 \in \arg\min_{K_i \in \mathcal{A}_h^{el}(a)} \tilde{n}_\sigma^a(K_i)$ and define $h^a := h_{K_1}$. For any $K_j \in \mathcal{A}_h^{el}(a)$, using the definition of the sequence $\mathcal{P}_h(a, K_1, K_j)$, we have:

$$\max_{K_j \in \mathcal{A}_h^{el}(a)} \frac{h_a}{h_{K_j}} = \max_{K_j \in \mathcal{A}_h^{el}(a)} \frac{h_{K_1}}{h_{K_{1j}^2}} \cdots \frac{h_{K_{1j}^{m-1}}}{h_{K_j}} \leqslant \sigma^{\tilde{n}_\sigma^a - 1}.$$

By its definition, $\tilde{n}_\sigma^a \leqslant n_\sigma^a$. Let us note that for nodes on faces $n_\sigma^a = 2$, and on interior nodes the same result applies for $n_\sigma^a = 1$. It proves the lemma. □

Let us define the δ-weighted norm $\|v\|_\delta := (v, v)_\delta^{\frac{1}{2}}$, with the definition of the δ-weighted inner product in (7) or (8), depending on the case considered. Finally, we note that $\nabla Q_h \subset D_h$, and so $\delta(i_h^\perp(\nabla p_h))$ is well-defined. In the next theorem, we state the stability of the numerical method (6). It relies on the following assumption, which is also required for the OSS method. We define $\pi_h^\perp(v) := v - \pi_h(v)$, where $\pi_h(v)$ has been defined in (9).

Assumption 5. For any $v_h \in D_h$

$$c_H \|v_h\|_\delta \leqslant \|\pi_h^\perp(v_h)\|_\delta + \|\pi_{h,0}(v_h)\|_\delta$$

for some $c_H > 0$ independent of h.

This assumption says that the δ-weighted projection of v_h on $V_h \cap V_{h,0}^\perp$ can be uniformly bounded by its $V_{h,0}$ and $V_h^\perp$ projections. We refer to [12] for the proof that this condition holds for simplicial meshes. The OSS formulation also relies on this assumption, as soon as we consider the projector $\pi_h(\cdot)$. Both OSS with $\pi_{h,0}(\cdot)$ and NPS with $i_{h,0}(\cdot)$ do not need this assumption anymore.

Theorem 6. *For the definition of the δ-product in (7) or (8), for any $p_h \in Q_h$*

$$\beta \|p_h\|_Q \leqslant \sup_{v_h \in V_{h,0}} \frac{(p_h, \nabla \cdot v_h)}{\|v_h\|_V} + \|i_h^\perp(\nabla p_h)\|_\delta$$

for some $\beta > 0$ independent of h.

Proof. Let us consider the numerical analysis for the element-wise case (7), since the one for the nodal-based case (8) is slightly simpler. Since $\delta(\pi_{h,0}(\nabla p_h)) \in V_{h,0}$ by construction, we get:

$$\begin{aligned} -(p_h, \nabla \cdot \delta(\pi_{h,0}(\nabla p_h))) &= (\nabla p_h, \delta(\pi_{h,0}(\nabla p_h))) \\ &= (\pi_{h,0}(\nabla p_h), \delta(\pi_{h,0}(\nabla p_h))) \\ &= \sum_{K \in \mathcal{T}_h} \sum_{a,b \in \mathcal{N}_h(K)} \delta_a \pi_{h,0}(\nabla p_h)^a \pi_{h,0}(\nabla p_h)^b (\phi^a, \phi^b)_K \\ &\gtrsim \|\pi_{h,0}(\nabla p_h)\|_\delta. \end{aligned}$$

We have used the definition of the projector (10) and the inequality $c_1^{-1}\delta_K \leqslant \delta_a \leqslant c_1 \delta_K$ for $0 < c_1 \leqslant \sigma^{2(n_\sigma - 1)}$, consequence of Lemma 4. Using the local inverse inequality (12), we get

$$\|\delta(\pi_{h,0}(\nabla p_h))\|_V^2 \leqslant \sum_{K \in \mathcal{T}_h} \nu h_K^{-2} \|\delta(\pi_{h,0}(\nabla p_h))\|_K^2 \lesssim \|\pi_{h,0}(\nabla p_h)\|_\delta.$$

Combining these results, we get:

$$\|\pi_{h,0}(\nabla p_h)\|_\delta \lesssim \sup_{v_h \in V_{h,0}} \frac{(p_h, \nabla \cdot v_h)}{\|v_h\|_V}.$$

Clearly, the stabilization term provides control over $(i_h^\perp(\nabla p_h), i_h^\perp(\nabla p_h))_\delta = \|i_h^\perp(\nabla p_h)\|_\delta^2$. Let us recall the following result, that follows from [14, Lemma 9.7] and the fact that $(\phi^a, \phi^a)_K \approx h_K^d$ for any $a \in \mathcal{N}_h(K)$. For any FE $K \in \mathcal{T}_h$ and any FE function $v_h \in D_h$

$$\begin{aligned} c_m^{-1} \sum_{a \in \mathcal{N}_h(K)} (v_h^a)^2 (\phi^a, \phi^a)_K &\leqslant \sum_{a,b \in \mathcal{N}_h(K)} v_h^a v_h^b (\phi^a, \phi^b)_K \\ &\leqslant c_m \sum_{a \in \mathcal{N}_h(K)} (v_h^a)^2 (\phi^a, \phi^a)_K \end{aligned} \tag{14}$$

for a constant $c_m > 0$ that does not depend on σ or h. We have:

$$\begin{aligned} \|\pi_h^\perp(\nabla p_h)\|_\delta^2 &\lesssim \sum_{K \in \mathcal{T}_h} \sum_{a \in \mathcal{N}_h(K)} \delta_K (\pi_h^\perp(\nabla p_h)^a)^2 (\phi^a, \phi^a)_K \lesssim (\pi_h^\perp(\nabla p_h), \delta(\pi_h^\perp \nabla p_h)) \\ &= (\pi_h^\perp(\nabla p_h), \delta(\pi_h^\perp(\nabla p_h)) + (\pi_h^\perp(\nabla p_h), \delta(\pi_h(\nabla p_h) - i_h(\nabla p_h)) \\ &= (\pi_h^\perp(\nabla p_h), \delta(i_h^\perp(\nabla p_h)) \\ &\lesssim \|\pi_h^\perp(\nabla p_h)\|_\delta \|i_h^\perp(\nabla p_h)\|_\delta, \end{aligned}$$

where we have used the relation $(\pi_h^\perp(\nabla p_h), w_h) = 0$ for any $w_h \in V_h$, obtained from (9). Combining these results with Assumption 5 we get:

$$\|\nabla p_h\|_\delta \lesssim \sup_{v_h \in V_{h,0}} \frac{(p_h, \nabla \cdot v_h)}{\|v_h\|_V} + \|i_h^\perp(\nabla p_h)\|_\delta. \tag{15}$$

Now, using the continuous inf–sup condition, for any $p_h \in Q$ there exists $v_p \in V_0$ with $\|v_p\|_V = 1$ such that $\beta \|p_h\|_Q \leqslant (p_h, \nabla \cdot v_p)$. Using the Scott–Zhang projector $i_{h,0}$ onto $V_{h,0}$ that satisfies homogeneous boundary conditions, we have:

$$\begin{aligned} \beta \|p_h\|_Q &\leqslant (\nabla p_h, v_p - i_{h,0}(v_p)) + (p_h, \nabla \cdot i_{h,0}(v_p)) \lesssim \|\nabla p_h\|_\delta \\ &\quad + \frac{|(p_h, \nabla \cdot i_{h,0}(v_p))|}{\|i_h(v_p)\|_V}, \end{aligned} \tag{16}$$

where we have used integration by parts, the interpolation estimate (13) and the stability of the Scott–Zhang projector (obtained from (13) for $k = s$). We prove the theorem invoking (15) in (16). The analysis for the nodal definition of δ in (8) follows in a similar way, with slight modifications. It is based on the fact that $(\delta^{\frac{1}{2}}(v_h), \delta^{\frac{1}{2}}(v_h)) \approx (v_h, \delta(v_h))$, which is a consequence of (14). □

The analysis for $i_{h,0}(\cdot)$ is straightforward and does not require Assumption 5. The following corollary is a direct consequence of this theorem and the coercivity of the viscous term $\nu(\nabla u, \nabla u) = \|u\|_V^2$.

Corollary 7. *The stabilized bilinear form $c_h(\cdot)$ defined in (6) and (7) (or (6)–(8)) satisfies*

$$\beta \leqslant \inf_{(u_h, p_h) \in V_{h,0} \times Q_h} \sup_{(v_h, q_h) \in V_{h,0} \times Q_h} \frac{c_h(u_h, p_h, v_h, q_h)}{(\|u_h\|_V + \|p_h\|_Q)(\|v_h\|_V + \|p_h\|_Q)}$$
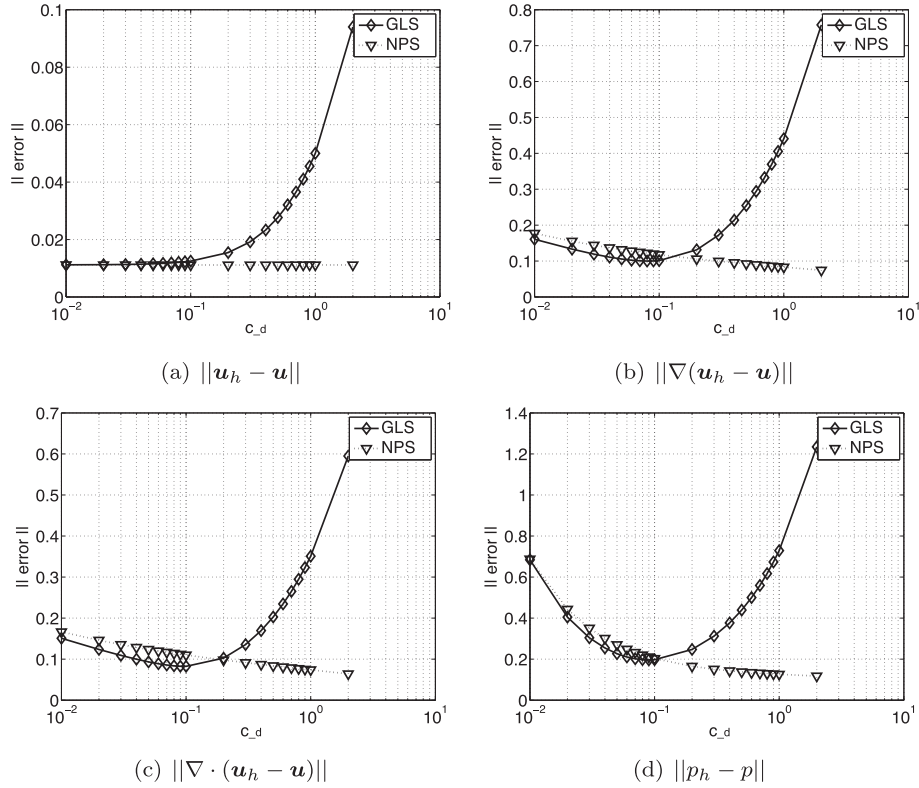
for some $\beta > 0$ independent of h.

3.2. Convergence analysis

Finally, we show that method (6) is optimally convergent.

Theorem 8. *The solution (u_h, p_h) of the discrete problem (6) and (7) (or (6)–(8)) satisfies:*

$$\begin{aligned} \|u - u_h\|_V + \|p - p_h\| &\lesssim \inf_{(w_h, r_h) \in V_{h,0} \times Q_h} (\|u - w_h\|_V + \|p - r_h\|_Q) \\ &\quad + \|i_h^\perp(\nabla p)\|_\delta. \end{aligned}$$

Fig. 2. Sensitivity of GLS/VMS and NPS methods for some error quantities with respect to the stabilization parameter constant c_δ. The mesh refinement level is $\ell = 6$.

Proof. Subtracting the continuous problem (2) and the discrete one (6), we easily obtain:

$$c_h(w_h - u_h, r_h - p_h, v_h, q_h) = c_h(w_h - u, r_h - p, v_h, q_h) + (i_h^\perp(\nabla p), i_h^\perp(\nabla q_h))_\delta \quad (17)$$

for any (w_h, r_h), $(v_h, q_h) \in V_{h,0} \times Q_h$. Using the local estimate in (13) with $k = l$ and the local inverse inequality (12), we have

$$\|i_h^\perp(\nabla r_h)\|_\delta^2 \lesssim \sum_{K \in \mathcal{T}_h} \delta_K \|\nabla r_h\|_{S_K}^2 \lesssim \sum_{K \in \mathcal{T}_h} \delta_K h_K^{-2} \|r_h\|_{S_K}^2 \lesssim \|r_h\|_Q^2. \quad (18)$$

This result can be used to prove the continuity of the bilinear form $c_h(w_h - u_h, r_h - p_h, v_h, q_h)$ in $V \times Q$, i.e.

$$c_h(w_h, r_h, v_h, q_h) \leqslant (\|w_h\|_V + \|r_h\|_Q) \times (\|v_h\|_V + \|q_h\|_Q),$$
$$\text{for any } (w_h, r_h), (v_h, q_h) \in V_{h,0} \times Q_h. \quad (19)$$

Finally, invoking the stability result in Corollary 7 and inequalities (18) and (19) in (17), we obtain:

$$\|w_h - u_h\|_V + \|r_h - p_h\|_Q \lesssim \|u - w_h\|_V + \|p - r_h\|_Q + \|i_h^\perp(\nabla p)\|_\delta.$$

Using the triangle inequality we prove the theorem. □

As a consequence, using e.g. the approximability properties of the Scott–Zhang projector, we have the following corollary.

Corollary 9. *Let us assume that the solution of the continuous problem (1) satisfies $(u, p) \in H^{1+\alpha}(\Omega) \times H^\alpha(\Omega)$ for some $\alpha \geqslant 1$. The solution (u_h, p_h) of the discrete problem (6) and (7) (or (6)–(8)) satisfies:*

$$\|u - u_h\|_V + \|p - p_h\| \lesssim h^\mu(v^{\frac{1}{2}}\|u\|_{H^{1+\mu}(\Omega)} + v^{-\frac{1}{2}}\|p - r_h\|_{H^\mu(\Omega)}),$$
$$\text{with } \mu := \min(r_u, r_p + 1, \alpha),$$

where r_u and r_p are the order of approximation of V_h and Q_h respectively.

4. Numerical experiments

4.1. h-convergence and c_δ-dependence

In order to test the convergence of the proposed method, we analyze its convergence towards the exact solution as $h \searrow 0$. We have considered the Stokes problem on the unit square with exact solution:

$$u(x, y) = (20xy^3, 5x^4 - 5y^4), \quad p(x, y) = 60x^2y - 20y^3.$$

This test problem has been proposed in [20] and also used in [5]. We have compared the GLS method, which coincides with VMS for linear FEs, and the NPS method in (6) and (7). We have used a family of regular triangular FE meshes with $h = 2^{-l}$, with $\ell = 1, 2, 3, 4, 5, 6$. For this test problems, the difference between choices (7) and (8) is not appreciable, since the family of meshes used in the convergence analysis are regular. The difference between the element-wise and nodal-wise definition of the stabilization parameter is expected to be more significant for non-degenerate meshes, i.e. using adaptive refinement, and remarkable for anisotropic meshes.

First of all, we have analyzed the sensitivity of both the GLS formulation (3) and the NPS formulation (6). In Fig. 2 we have plotted some quantities of the velocity and pressure error with respect to c_δ. The GLS method has an optimal behavior at $c_\delta \sim 0.1$ for all quantities, but increasing c_δ has a clear negative impact on accuracy. On the contrary, the NPS formulation is quite insensitive to c_δ; this behavior is particularly relevant for the L^2-norm of the velocity error in Fig. 2(a). Further, the NPS formulation seems to sligthly improve for larger values of c_δ.

Taking the optimal value $c_\delta = 0.1$ for the GLS formulation, we have plotted the error against the mesh size h in Fig. 3 for both methods. We observe an almost identical behavior for both formulations. Optimal quadratic convergence is attained for the L^2-norm of the velocity error, and a super-convergence order of $\frac{3}{2}$ is observed for the rest of quantities.
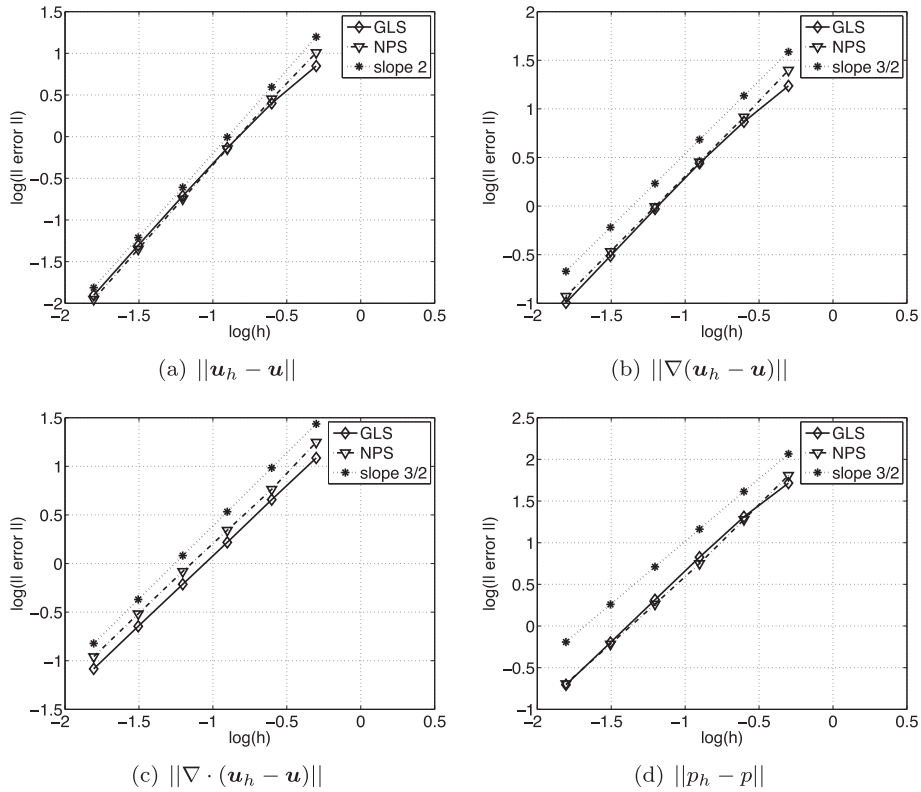
(a) $||\boldsymbol{u}_h - \boldsymbol{u}||$

(b) $||\nabla(\boldsymbol{u}_h - \boldsymbol{u})||$

(c) $||\nabla \cdot (\boldsymbol{u}_h - \boldsymbol{u})||$

(d) $||p_h - p||$

Fig. 3. Convergence analysis of GLS/VMS and NPS methods for some error quantities.
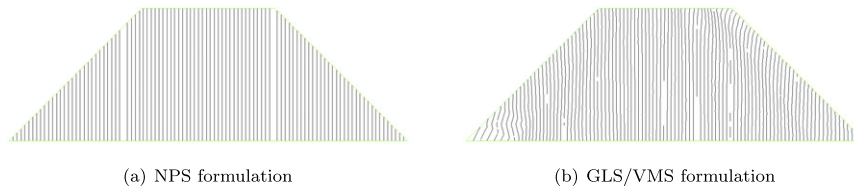

(a) NPS formulation

(b) GLS/VMS formulation

Fig. 4. Contour lines of the pressure field for the Poiseuille flow test.

4.2. Pressure error on the boundary

The artificial pressure boundary layers that appear with GLS/VMS formulations are well-known. Let us consider the Poiseuille flow test in [12] for a structured mesh of 1,250 linear triangular FEs; we refer to this work for a complete discussion about the misbehavior of the GLS/VMS formulation. We show the pressure contours for both formulations in Fig. 4. The GLS/VMS formulation produces a wrong solution, motivated by the fact that $\partial_n p = 0$ is weakly enforced on the boundary. On the other hand, even though $u \notin V_h$, the NPS solution leads to the exact pressure, as the LPS formulation in [5] (see this reference for a super-convergence proof).

5. Conclusions

In this work, we have considered a symmetric stabilization method based on a non-standard version of the Scott–Zhang projector that is well-posed for $L^1(\Omega)$ functions. This low regularity requirement is needed, in order to project FE pressure gradients, which are discontinuous element-wise polynomials. Further, the application of this projector over this type of functions is very simple and cheap and allows for an efficient implementation of the method.

This projector has important benefits compared to the existing choices: the $L^2(\Omega)$ projector in OSS [12] and the local projections in LPS techniques [5,19]. On one hand, the projector is local, i.e. no global linear system must be solved to compute the projections. It allows to explicitly have the system matrix in memory, which is required e.g. for ILU preconditioning of the full FE system matrix, the use of direct solvers or substructuring domain decomposition techniques for parallelization. Further, for iterative solvers, a global projector requires nested solvers, one for the FE problem and another one (per iteration) for the projection computation. So, the local projection is very desirable in order to facilitate implementation, reduce CPU cost and work on distributed memory machines. In particular, the extended stencil of the proposed method seems to be minimal. On the other hand, the proposed method lightens the requirements of LPS techniques, since it does not require any particular macro-element topology of the mesh or bubble-enriched FE spaces.

Different alternatives of the method have been proposed, depending on the nature of the stabilization parameter (nodal vs. element definition) and the enforcement of Dirichlet boundary conditions in the projector. Some implementation issues have been addressed. Numerical analysis shows optimal stability and convergence properties, which have also been checked via numerical

experimentation. Compared to the GLS/VMS formulations, the resulting method is less sensitive to the choice of the stabilization parameter and does not exhibit the pressure misbehavior on the boundary.

The method has been presented for the Stokes problem. However, we can apply it to Darcy's or Maxwell's systems, using the ideas in [2], by replacing the $L^2(\Omega)$ projections by the Scott–Zhang projector proposed herein.

Acknowledgements

References

[1] S. Badia, R. Codina, Unified stabilized finite element formulations for the Stokes and the Darcy problems, SIAM Journal on Numerical Analysis 47 (3) (2009) 1971.

[2] S. Badia, R. Codina, Stokes, Maxwell and Darcy: a single finite element approximation for three model problems, Applied Numerical Mathematics 62 (4) (2012) 246–263.

[3] S. Badia, R. Codina, R. Planas, On an unconditionally convergent stabilized finite element approximation of resistive magnetohydrodynamics, UPcommons (2011). http://www.hdl.handle.net/2117/15755.

[4] S. Badia, R. Planas, J.V. Gutiérrez-Santacreu, Unconditionally stable operator splitting algorithms for the incompressible magnetohydrodynamics (MHD) system discretized by a stabilized finite element formulation based on projections, International Journal for Numerical Methods in Engineering (2012), in press, http://dx.doi.org/10.1002/nme.4392.

[5] R. Becker, M. Braack, A finite element pressure gradient stabilization for the Stokes equations based on local projections, Calcolo 38 (4) (2001) 173–199.

[6] S.C. Brenner, R. Scott, The Mathematical Theory of Finite Element Methods, Springer, 2010.

[7] H. Brezis, Functional Analysis Sobolev Spaces and Partial Differential Equations, Springer, 2010.

[8] F. Brezzi, M. Fortin, Mixed and Hybrid Finite Element Methods, Springer-Verlag, 1991.

[9] P.G. Ciarlet, The Finite Element Method for Elliptic Problems, second ed., SIAM: Society for Industrial and Applied Mathematics, 2002.

[10] Ph. Clément, Approximation by finite element functions using local regularization, ESAIM: Mathematical Modelling and Numerical Analysis 9(R2) (1975).

[11] R. Codina, Stabilized finite element approximation of transient incompressible flows using orthogonal subscales, Computer Methods in Applied Mechanics and Engineering 191 (39–40) (2002) 4295–4321.

[12] R. Codina, J. Blasco, A finite element formulation for the Stokes problem allowing equal velocity–pressure interpolation, Computer Methods in Applied Mechanics and Engineering 143 (3-4) (1997) 373–391.

[13] R. Codina, Javier Principe, Oriol Guasch, S. Badia, Time dependent subscales in the stabilized finite element approximation of incompressible flow problems, Computer Methods in Applied Mechanics and Engineering 196 (21–24) (2007) 2413–2430.

[14] A. Ern, J.-L. Guermond, Theory and Practice of Finite Elements, Springer, 2004.

[15] V. Girault, J.-L. Lions, Two-grid finite-element schemes for the transient Navier–Stokes problem, ESAIM: Mathematical Modelling and Numerical Analysis 35 (5) (2002) 945–980.

[16] T.J.R. Hughes, L.P. Franca, M. Balestra, A new finite element formulation for computational fluid dynamics: V. Circumventing the Babuska–Brezzi condition: a stable Petrov–Galerkin formulation of the stokes problem accommodating equal-order interpolations, Computer Methods in Applied Mechanics and Engineering 59 (1) (1986) 85–99.

[17] T.J.R. Hughes, Multiscale phenomena: Green's functions, the Dirichlet-to-Neumann formulation, subgrid scale models, bubbles and the origins of stabilized methods, Computer Methods in Applied Mechanics and Engineering 127 (1-4) (1995) 387–401.

[18] K.E. Jansen, S.S. Collis, C. Whiting, F. Shakib, A better consistency for low-order stabilized finite element methods, Computer Methods in Applied Mechanics and Engineering 174 (1–2) (1999) 153–170.

[19] G. Matthies, P. Skrzypacz, L. Tobiska, A unified convergence analysis for local projection stabilisations applied to the Oseen problem, ESAIM: Mathematical Modelling and Numerical Analysis 41 (4) (2007) 713–742.

[20] S. Norburn, D. Silvester, Stabilised vs. stable mixed methods for incompressible flow, Computer Methods in Applied Mechanics and Engineering 166 (1-2) (1998) 131–141.

[21] R. Planas, S. Badia, R. Codina, Approximation of the inductionless MHD problem using a stabilized finite element method, Journal of Computational Physics 230 (8) (2011) 2977–2996.

[22] D. Schötzau, Mixed finite element methods for stationary incompressible magneto-hydrodynamics, Numerische Mathematik 96 (4) (2004) 771–800.

[23] L.R. Scott, S. Zhang, Finite element interpolation of nonsmooth functions satisfying boundary conditions, Mathematics of Computation 54 (190) (1990) 483–493.

[24] F. Shakib, T.J.R. Hughes, A new finite element formulation for computational fluid dynamics: IX. Fourier analysis of space-time Galerkin/least-squares algorithms, Computer Methods in Applied Mechanics and Engineering 87 (1) (1991) 35–58.

[25] A. Toselli, O. Widlund, Domain Decomposition Methods, first ed., Springer, 2004.